Dissociative-recombination and excitation measurements with H_2^+ and HD^+

L. H. Andersen, P. J. Johnson, D. Kella, H. B. Pedersen, and L. Vejby-Christensen
Institute of Physics and Astronomy, University of Aarhus, DK 8000, Aarhus C, Denmark
(Received 9 October 1996)

The cross sections for dissociative recombination (DR) and dissociative excitation (DE) have been measured for the H_2^+ and HD^+ molecular ions in the energy range from 0 to ~30 eV. An imaging technique that provides a measure of the kinetic energy release in the DR process was used to yield information about the initial vibrational distribution of the molecular ions and the final atomic states of the DR reaction. The results for DR with HD^+ in the vibrational ground level, $\nu=0$, are compared with other measurements and recent multichannel quantum defect theory calculations. Significant deviations that appear at high energy ~5–10 eV are discussed. The present work reports on an absolute DE measurement with HD^+. The vibrational distribution of H_2^+ was manipulated by photodissociation of ions in vibrationally excited levels. We obtained DE and DR cross sections for H_2^+ ions populating primarily the two lowest vibrational levels $\nu=0,1$ and H_2^+ ions in a broad vibrational distribution. It is found that DR of H_2^+ with zero energy electrons results in the $H(n=1)+H(n=2)$ final channel, open for all vibrational levels, and in the $H(n=1)+H(n=3)$ channel, which is energetically open for initial vibrational levels $\nu \geq 5$. [S1050-2947(97)00204-7]

PACS number(s): 34.80.Lx, 29.20.Dh, 34.50.−s, 34.80.Gs,

I. INTRODUCTION

The dissociative-recombination (DR) process for a diatomic molecular ion may be written as

$$AB^+(\alpha,\nu,J)+e_E^-\rightarrow A^0(n_1)+B^0(n_2)+\Delta E_k, \qquad (1)$$

where a molecular ion in the electronic state α, vibrational level ν, and rotational state J captures a free electron and dissociates into two atoms in quantum states n_1 and n_2. ΔE_k is the kinetic energy release, which depends on the electronic excitation of the atoms (n_1,n_2), the kinetic energy (E) of the incoming electron in the rest frame of the molecular ion, and the initial state of the molecular ion. Dissociative excitation (DE) for a diatomic ion may be written as

$$\begin{aligned} AB^+(\alpha,\nu,J)+e_E^- &\rightarrow A^+ + B^0 + e^- + \Delta E_k \\ &\rightarrow A^0 + B^+ + e^- + \Delta E_k. \end{aligned} \qquad (2)$$

The DR and DE processes involve transformation of potential and kinetic energy from the incoming electron into kinetic energy of the nuclei after dissociation of the molecule. To understand the DR and DE processes, knowledge is required about the initial potential-energy curves of the molecular ion and the repulsive curves of the excited, neutral molecule. Such energy curves are based on the Born-Oppenheimer approximation. Moreover, the capture probability of the relevant curves and the progression along the repulsive curves, often with many level crossings to the final atomic limits, must be understood. Some aspects of the recombination process such as couplings without curve crossings and excitation of the vibrational motion by the incoming electron requires a treatment which is beyond the Born-Oppenheimer approximation, and experimental studies of DE and DR provide a way to improve our ability to treat the various difficult aspects of the molecular processes.

From an applicational point of view, it is of major concern to have information about the degree of electronic excitation of the atomic fragments and accurate knowledge about the cross sections as a function of energy (E). Dissociative recombination has been studied with a variety of different ions of astrophysical and atmospheric interest. An important example is DR of O_2^+, which can produce free oxygen atoms in the excited ^1S state, which may cause the green line at 5577 Å, a prominent feature of the spectrum of the Earth's night sky [1,2]. Another example is DR of N_2^+, which plays an important role for the isotope composition in the atmosphere of Mars [3,4]. For polyatomic molecules it is, in addition, of crucial importance to know the chemical composition of the neutral dissociation fragments in the final state. Recently, such branching ratios of astrophysical relevance have been obtained for H_3^+ [5] and H_3O^+ [6].

The field of electron-molecular ion scattering at low energy has advanced considerably over the last couple of years due to the utilization of heavy-ion storage rings; see, e.g, Ref [7]. In the rings, the so-called electron coolers are being used to provide electrons with a narrow velocity distribution for merged-beam experiments. At low relative energy, the energy resolution typically corresponds to 10–100 meV in the rest frame of the molecular ion [8]. The storage rings are being used to provide energetic molecular ions, the dissociation products of which are easily detected by single-particle counters. To obtain the highest level of information from experiments, the population of the initial electronic, vibrational, and rotational states should be known. Experimentally, this is a major challenge. Most work has been done with molecular ions in their electronic and vibrational ground state. In the rings, cold molecular ions are normally achieved by storing the molecular species for several seconds before the measurement begins. However, for diatomic molecular ions this method only works when the molecular ion has a dipole moment large enough to allow vibrational and rotational internal cooling to take place. Homonuclear, diatomic molecular ions do not cool down since they have no permanent dipole moment. In this case one may use the long storage time of tens of seconds to actively get a control of

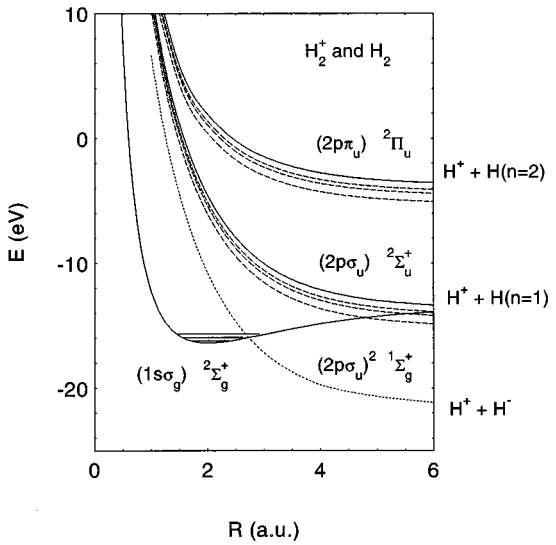

FIG. 1. Some potential energy curves for H_2^+ and HD^+. Solid lines are potential curves of the molecular ion, and dashed lines represent states of the neutral molecule. For more details, see Ref. [10]. The vibrational spacing is shown for H_2^+.

the vibrational distribution, e.g., by lasers. The first experiment with such an active control was recently performed at the Aarhus Storage Ring, Denmark (ASTRID) [9].

The present study deals with two one-electron molecular ions, H_2^+ and HD^+. These ions have received special attention in relation to DR because of their obvious importance in many plasma environments and because they provide an excellent test of theory. Although the molecular hydrogen ions have been subject to several theoretical and experimental DE and DR studies, and some relevant excited-state potential curves of H_2 have been calculated [10] (see Fig. 1), the processes are far from being completely understood. The HD^+ molecular ion quickly relaxes by infrared emission, and the results reported here are with ions in the vibrational ground state $\nu=0$. The H_2^+ ion, however, does not spontaneously relax neither vibrationally nor rotationally. In this work, we used a photodissociation technique to remove vibrationally hot ions and obtained a beam of H_2^+ ions with mainly $\nu=0$ and 1 populated:

$$h\nu + H_2^+(\nu>1) \rightarrow H^+ + H(n=1). \tag{3}$$

An imaging technique was used to provide direct information about the *initial* vibrational state of H_2^+. In earlier experiments, such information has been derived from the assumed chemistry in the ion source or from the shape of the obtained DR cross section [9,11]. The imaging technique also provides information about the *final* electronic states of the hydrogen atoms after DR.

DR cross sections with the molecular hydrogen ion and its isotopes were first measured in the mid 1970s [12–17]. A significant population of the vibrationally excited states in the molecular ion beam was due to the production method of electron-impact ionization of H_2. Later, the low-energy region ($E<1$ eV) was considered in a single-pass experiment [18,19] where the vibrational distribution of H_2^+ was estimated to be limited to $\nu=0$, 1, and 2 by operating the ion source under special conditions. More recently, DR cross sections of HD^+ and H_2^+ were measured at heavy-ion storage rings; at TSR [20,21], TARN II [22], and ASTRID [9], but no absolute cross sections were determined. It has been proved by an imaging technique that only $\nu=0$ was populated in the HD^+ beam at TSR [23]. Compared with the HD^+ data, a much broader structure appeared in the H_2^+ data (cross section *versus* energy), indicating that many vibrationally excited states were involved for this molecular ion at TSR [24]. At CRYRING, DR of D_2^+, H_2^+, and HD^+ has been measured [11,25,26]. Of all the previous work on DR with HD^+, only the experiment at CRYRING [26] yielded cross sections on an absolute scale.

Several theoretical papers on DR with H_2^+ and HD^+ exist [26–34], and the low-energy region ($E<1$ eV) has in particular attracted a great deal of attention. The combination of a direct electron-capture transition from the electronic ground state $(1s\sigma_g)$ to the $(2p\sigma_u)^2$ state (see Fig. 1) and recombination involving vibrational excitation and capture to the $(1s\sigma_g)nl\lambda$ Rydberg states results in narrow structures in the cross section [30,31,33,35,36]. At high energy, above 1 eV, only little theoretical work has been done [26–28,34]. Primarily, capture to low Rydberg states of an excited $(2p\sigma_u)$ core has been considered. Calculations for HD^+ that included the effect of rotations [22,34] showed good agreement with measurements from the TARN II storage ring [22] on a relative scale.

There has been substantial experimental DE work on vibrationally hot H_2^+ [37–42], but not with cold vibrationally controlled H_2^+. The observed discrepancy between experimental data [43] may be related to different vibrational distributions in the experiments. The DE cross section behavior near threshold was used in an attempt to obtain information about the vibrational distribution of H_2^+, for a DR measurement [18]. The DE data appeared to have a threshold corresponding to the energy needed for the direct transition from vibrational levels of the electronic ground state to the first repulsive curve of the ion. But, as will be shown in the present paper, the DE cross section is non-negligible below this energy. Thus, there was no direct measurement of the vibrational distribution in the early work by Hus *et al.* [18], and there still is a lack of absolute DE and DR cross-section measurements with H_2^+ molecular ions that have been proven to be cold.

The DE process is difficult to treat theoretically because the final state involves both an electronic and a dissociation continuum. References to theoretical work on DE with molecular hydrogen ions and their isotopes are very scarce; the reader is referred to a paper by Takagi [44] and a paper relevant to high-energy impact by Peek [45], which deals with the problem in the first Born approximation.

In the present work, we provide absolute DR and DE cross sections for $HD^+(\nu=0)$ as well as for vibrationally hot and cold H_2^+. In the following we first discuss the experiment, and then the data.

II. EXPERIMENT

The present experiment was carried out at the ASTRID storage ring [46] (see Fig. 2). The ring is 40 m in circumference and has two 45° bending magnets in each of the four

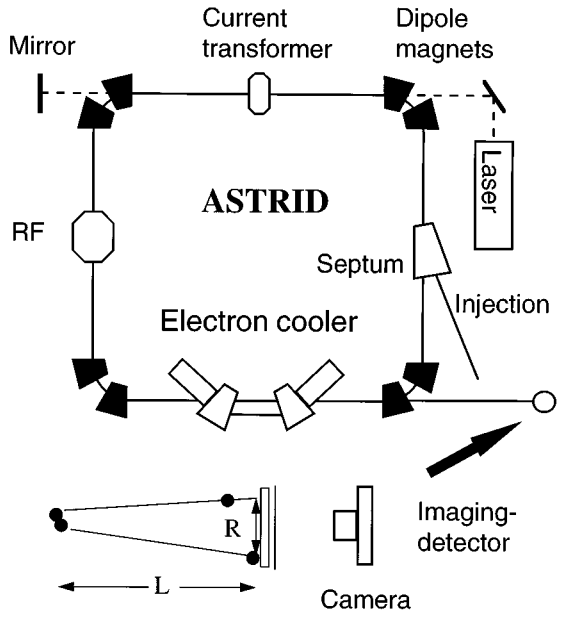

FIG. 2. The ASTRID storage ring with the principle of the imaging detector.

corners. The H_2^+ ions were produced in a plasma-type ion source by electron-impact ionization of H_2 [47], and the HD^+ ions in a RF source. Measurements on HD^+ ions were made after they had been injected into the ring at 150 keV and accelerated to 2.87 MeV. Injection and acceleration were accomplished in about 3 s. The H_2^+ beam was also injected at 150 keV. However, to achieve a large Doppler shift of the applied laser light for photodissociation (see later discussion), the beam was accelerated to 43 MeV and kept at this energy for 10 s before being decelerated to 2.97 MeV, at which energy the DE and DR measurements were done. The average pressure in the ring was $\sim(3–5)\times10^{-11}$ mbar, and the beams had storage lifetimes of about 5–10 s.

The molecular-ion beams were merged with an almost monoenergetic beam of electrons from the electron cooler, which has been described previously [48,49]. Different relative energies E were obtained by varying the electron-beam energy, which was typically 500–1000 eV in the laboratory frame. The electron beam had a diameter of 2.5 cm and was guided by a ~200-G magnetic field, which was applied to compensate for the space-charge field of the electrons.

A. Cross sections

Neutral particles produced by DR and DE in the electron beam were detected behind the dipole magnet after the electron cooler (see Fig. 2). We used an energy-sensitive 1200-mm^2 solid-state detector (SSD) to discriminate between the case of DE where the detector is hit by one neutral atom and that of DR where it is hit by two. Experimentally, we determined the DR rate coefficient for HD^+ as

$$\langle v\sigma\rangle = \frac{N(H^0+D^0)-N_0(H^0+D^0)}{N(HD^+)}\,\frac{v_i}{\Delta L\rho\epsilon}, \tag{4}$$

where v is the relative velocity, σ the cross section, ϵ (=1) the ion-detection efficiency, v_i the ion velocity, ΔL the cooler length, and ρ the electron density. $N(H^0+D^0)$ is the yield of particles recorded by the SSD at the energy corresponding to two neutrals, $N_0(H^0+D^0)$ is the contribution from collisions with the background gas (essentially zero), and $N(HD^+)$ is the number of beam particles per second passing through the interaction region. We used a beamcurrent transformer capable of measuring a bunched ion-beam current down to about 50 nA. In a similar way we determined a DE rate coefficient by counting only one neutral (H or D). The rate coefficients of H_2^+ were obtained in an analogous way. To avoid acceleration of ions during the measurement caused by the drag force from the electrons, the relative electron-beam energy was modulated between 0 (cooling) and the energy E (measuring). In this way, the rate coefficient for recombination at the energy E was measured relative to the rate coefficient at $E=0$. At $E=0$ the absolute DR rate coefficient was measured by turning the electron beam on and off at a frequency of 25 Hz. The experimental uncertainty on the absolute rate coefficient is estimated to be $\pm20\%$, with the main contribution coming from the ion-current measurement.

The measured rate coefficient may be compared with theory when the theoretical cross section σ is known:

$$\langle v\sigma\rangle = \int v\sigma(v)f(v)dv. \tag{5}$$

The electron-velocity distribution function $f(v)$ is given by [48]

$$f(v)=\left(\frac{m}{2\pi kT_\perp}\right)e^{-mv_\perp^2/2kT_\perp}\left(\frac{m}{2\pi kT_\parallel}\right)^{1/2}e^{-m(v_\parallel-\Delta)^2/2kT_\parallel}, \tag{6}$$

where $v_\perp$ and $v_\parallel$ are the electron-velocity components respectively perpendicular to and parallel to the ion-beam direction, and Δ is the detuning velocity given by

$$\Delta=|\sqrt{(m/M)E_i}-\sqrt{E_e}|, \tag{7}$$

where m is the electron mass, M the mass of the molecular ion, and E_i and E_e the laboratory kinetic energy of the ions and electrons, respectively. We applied adiabatic expansion of the electron beam, and the expected temperatures are $kT_\perp=0.02$ eV and $kT_\parallel=10^{-4}-10^{-3}$ eV.

Throughout this paper cross sections were obtained as $\langle\sigma\rangle=\langle v\sigma\rangle/\Delta$. A significant difference between $\langle\sigma\rangle$ and the true cross section σ with the present electron-beam temperatures is found only at low relative energies (with a cross section being proportional to $1/E$, $\langle\sigma\rangle/\sigma\sim0.95$ at 0.1 eV and $\langle\sigma\rangle/\sigma\sim0.7$ at 0.01 eV).

B. Corrections to the cross section

In the electron cooler the ions travel parallel to the electron beam in the ~1-m interaction region. In this region, the relative velocities are well defined. In the two toroidal regions, where the beams join and separate, relative energies in the range of 0–20 eV may be encountered even with zero relative energy in the straight interaction region. Thus, when a small cross section appears at some relative energy E, with subsequent small signal rates from the interaction region, a

non-negligible signal may appear owing to a finite cross section at the energies encountered in the toroids. After achieving the measured total rates from the interaction region and the toroidal regions, a correction to the cross section was performed by subtracting a calculated contribution from the toroidal regions.

C. Imaging

To provide information about the population of the vibrational and rotational states in the beam as well as in the final atomic states, we used an imaging technique similar to that employed by Zajfman *et al.* [23]. Our imaging apparatus has also been used to measure branching ratios for DR of O_2^+ [2] and N_2^+ [4]. A measurement of the spatial separation between the dissociation fragments yield information about the kinetic energy release (ΔE_k) in the DR process. This separation was measured after a bending magnet (see Fig. 2) by a 77-mm-diameter microchannel-plate detector with a phosphor anode. The light from the phosphor anode was recorded by a charge-coupled device camera. By this technique we demonstrated that HD^+ ions reached their vibrational ground state with only little rotational excitation. We also measured the vibrational distribution of the H_2^+ beam both with and without the application of a ''cooling'' laser. This is discussed later.

To analyze the imaging data, we used the following formulation: Let E_i be the kinetic energy of the molecular ion at the time of recombination, θ the angle between the internuclear axis and the beam direction, and L the distance from the place of recombination to the imaging detector. Then the distance (R) measured on the detector

$$R=\left(\frac{\Delta E_k}{E_i}\right)^{1/2}\frac{m_1+m_2}{\sqrt{m_1 m_2}}\,L\,\sin\theta=R_{\max}\sin\theta, \tag{8}$$

where m_1 and m_2 are the masses of the atomic fragments. Since the imaging data were all taken at zero relative velocity, we assume an isotropic distribution in the rest frame of the molecular ion. After integration over the finite interaction length ΔL (about 1 m), we obtain the following expression for the distribution of distance between fragments [4]:

$$F(R)=\frac{1}{c\Delta L}\left(\arctan\frac{K(L_2)}{R}-\arctan\frac{K(L_1)}{R}\right), \tag{9}$$

where $L_1=L_0-L/2$, $L_2=L_0+L/2$, and $K(L_i)=\mathrm{Re}[(cL_1)^2-(R^2)]^{1/2}$, L_0 being the distance from the center of the interaction region to the imaging detector (613 cm) and $c=R_{\max}/L$. Equation (9) describes the shape of the distribution of projected distances for a single value of the kinetic-energy release.

In the present work we deal with rotationally excited ions by assuming that the cross section has negligible rotational dependence and that the rotational population is given by a Boltzmann distribution, with a single temperature T, independent of the vibrational excitation. If the population of the vibrationally excited levels is given by the function $p(\nu)$, the final distribution of projected distances becomes [4]

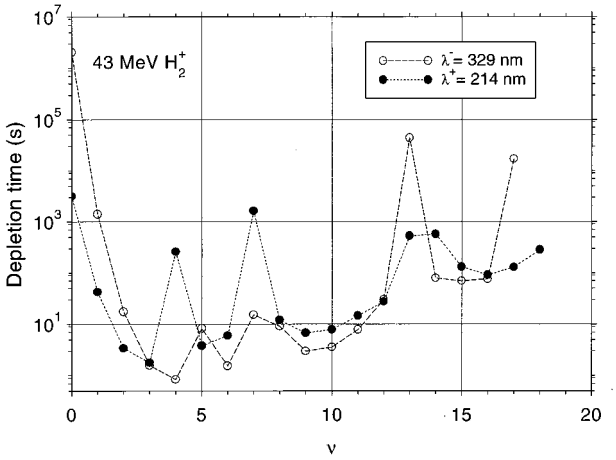

FIG. 3. Photodissociation-depletion times at the two Doppler-shifted frequencies at 43 MeV as a function of the vibrational quantum number of H_2^+. A beam overlap of 50% was assumed.

$$D(R)=\sum_J (2J+1)e^{-J(J+1)B/kT}\sum_\nu \sum_{f=n,n'} P(\nu,f)F(R), \tag{10}$$

where B is the rotational constant, f the final electronic channel of the dissociation products, and $P(\nu,f)=\mathrm{const}\times p(\nu)\langle v\sigma_{\nu,f}(v)\rangle$, where $\langle v\sigma\rangle$ is the rate coefficient defined above. The function $D(R)$ may be used to fit the experimentally obtained imaging data with kT and $P(\nu,f)$ as fitting parameters.

D. Laser manipulation

To perform an *active* control of the number of vibrational states populated in the H_2^+ beam, we applied laser light at 266 nm from a pulsed Nd:YAG laser, using fourth harmonic generation. The laser light was pulsed (8 ns pulses) with a repetition rate of 10 Hz and a pulse energy of about 100 mJ. The stored H_2^+ ions were successively bombarded by photons from the time of their injection into ASTRID. The 266-nm laser light was sent into the storage ring both parallel and antiparallel to the molecular-beam direction in one of the four straight sections; see Fig. 2. In this way the laser light interacted with stored ions over a section of about 2×8 meter. In the rest frame of 43 MeV H_2^+, two Doppler-shifted wavelengths, 329 and 214 nm, were obtained.

The photodissociation cross section exhibits dips at certain frequencies [50]. This results in anomalously long dissociation times for certain vibrational levels (defined as the time needed to bring the population for a given vibrational level down by a factor e^1). In Fig. 3, we show calculated dissociation times of the vibrational levels of H_2^+ for the two particular wavelengths. It is seen that the redshifted light is efficient for the few levels where the blueshifted light is inefficient. Assuming an overlap of 50% between the laser beam and the ion beam, it is calculated that mainly levels with $\nu=0$ and 1 will survive the 10-s irradiation at 43 MeV. At the time of the recombination measurement (20–30 s after injection), one might expect a population with 32% in $\nu=0$ and 68% in $\nu=1$ if the population from the ion source is given according to the Franck-Condon distribution [51], and

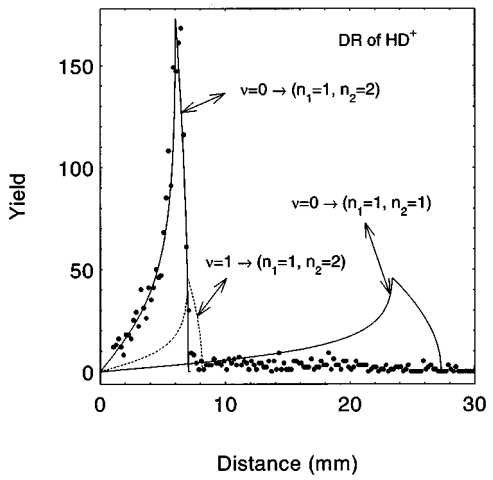

FIG. 4. Yield of pairs of H and D atoms following DR with HD^+ as a function of the projected distance on the detector, recorded at $E=0$.

all molecules in levels with $\nu>1$ are photodissociated.

E. Destruction of Rydberg states

In the dipole bending magnets the strong magnetic field perpendicular to the direction of motion of the ions results in a relatively strong electric field in the rest frame of the ions. The strength is

$$E' = \gamma\beta c B_\perp , \tag{11}$$

where $B_\perp$ is a magnetic field component perpendicular to the beam direction, $\beta = v_i/c$ is the ion speed divided by the speed of light, and γ equals $(1-\beta^2)^{-1/2}$ [52]. At 3 MeV, the ions have a velocity of about 5% of the speed of light and the induced electric field is about 50 kV/cm. The neutral atoms (H^0 and D^0) produced as a result of DE and DR are passed through the strong magnetic field and, as a consequence, the highest-lying Rydberg states are field ionized. Therefore, only Rydberg states with a principal quantum number n smaller than some n_{max} are detected. In the present experiment $n_{max}=10$. The flight time from the electron cooler to the magnet is 230 ns for H_2^+ and 290 ns for HD^+ and only atoms in the $11p$ level with a lifetime of 247 ns may decay a significant amount before reaching the magnet, and hence some atoms in this particular state may be counted as neutrals despite the fact that $n=11>n_{max}$.

III. RESULTS AND DISCUSSION

A. Imaging of HD^+

The imaging technique was used to establish that HD^+ reaches the vibrational ground level, as was also seen in an other storage-ring experiment [23]. Figure 4 shows the yield of pairs of H and D atoms as a function of their projected distance on the detector. The spectrum was taken after more than 5 s of storage, and the electron beam had zero kinetic energy in the rest frame of the molecular ions. There is only one peak, which is ascribed to the reaction $e^- + HD^+(\nu=0,J) \rightarrow H(n=1)+D(n=2)$ [or $D(n=1)+H(n=2)$]. The solid curve is the expected distribution for $J=0$, based on the assumption of isotropic emission [Eq. (9)]. For comparison the expected distribution for $e^- + HD^+(\nu=1,J=0) \rightarrow H(n=1)+D(n=2)$ [or $D(n=1)+H(n=2)$] is shown as well as for $e^- + HD^+(\nu=0,J=0) \rightarrow H(n=1)+D(n=1)$ [or $D(n=1)+H(n=1)$]. As seen from the figure, the initial vibrational level as well as the final atomic states are easily resolved, and for HD^+ only the $H(n=1)+D(n=2)$ [or $D(n=1)+H(n=2)$] channel is important, as expected from the potential energy curves and recently also seen in another experiment [23]. Since the data may satisfactorily be described with $J=0$, we conclude that the ions have relaxed rotationally, presumably to room temperature.

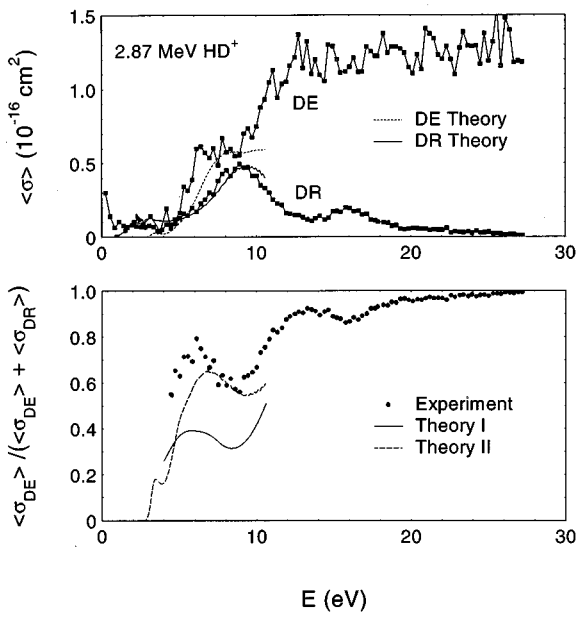

FIG. 5. Upper part: Averaged DE and DR cross sections $\langle\sigma\rangle = \langle v\sigma\rangle/v$ as a function of energy for HD^+ in the ground vibrational level. The data were recorded after 10 s of storage and have been corrected for the contributions in the toroidal regions. Shown are recent MQDT calculations of Takagi [53]. Lower part: The ratio $\langle\sigma_{DE}\rangle/(\langle\sigma_{DE}\rangle+\langle\sigma_{DR}\rangle)$ as a function of energy. Theory I is the MQDT calculation by Takagi [44]. Theory II is from [53].

1. DE of HD^+

Cross sections for DE and DR of $HD^+(\nu=0)$ are shown in the top part of Fig. 5. The cross sections were corrected for the contributions from the regions where the electron beam and ion beam join and separate. The correction ($\Delta\sigma/\sigma$) for the DE cross section is about 20% above 10 eV. For DR, the correction is a few percent at low energy ($E<0.1$) and about 10% above 8 eV. In the energy interval where the DR cross section is small (0.1 to 5 eV), the signal originating from the toroidal regions is, however, of the same magnitude as that from the section where the beams are parallel. The DR cross section will be discussed in detail later.

We found that the two DE channels of Eq. (2) were of equal strength, and in the remaining part of this paper the DE cross section refers to the sum of the two possible channels. As expected, the DE cross section is zero below the dissociation energy, which is 2.67 eV for HD^+ in the vibrational ground level [54]. However, the cross section is significant

at an energy smaller than the vertical energy difference between the initial state $(1s\sigma_g)\ ^2\Sigma_g^+(\nu=0)$ and the lowest dissociating curve $(2p\sigma_u)\ ^2\Sigma_u^+$, which is about 9 eV at the classical outer turning point (see Fig. 1). This implies that below ~9 eV DE proceeds via states that lie in the $e^- + H_2^+(1s\sigma_g)$ electronic and nuclear continua, which include doubly excited states of the neutral molecule. Hence, resonant electron capture to doubly excited states followed by autoionization into the dissociation continuum of the $^2\Sigma_g^+$ electronic ground state of HD^+ may be important. This mechanism was invoked to describe dissociative ionization of H_2 many years ago [55,56], and may also play a significant role in DE [57].

If the DE process proceeds dominantly by electron capture to doubly excited electronic states below the 9-eV threshold, it is the autoionization probabilities of these states that determine the magnitude of the DE as well as the DR cross sections. Important aspects of the DE process may be revealed when the ratio between the DE cross section and the DE cross section plus the DR cross section $[\sigma_{DE}/(\sigma_{DE}+\sigma_{DR})]$ is considered. Assuming that the processes can be described as a capture process followed by autoionization and dissociation in the case of DE, or followed by dissociation without autoionization in the case of DR, the ratio below the 9 eV threshold may be written as

$$\frac{\sigma_{DE}}{\sigma_{DE}+\sigma_{DR}} = \frac{\sum_i \sigma_c(i)\Gamma_{AD}(i)}{\sum_i \sigma_c(i)[\Gamma_{AD}(i)+\Gamma_D(i)]}, \qquad (12)$$

where $\sigma_c(i)$ is the capture cross section into level i, $\Gamma_{AD}(i)$ and $\Gamma_D(i)$ are the corresponding decay probabilities for autoionization plus dissociation and dissociation, respectively. Note that $\Gamma_{AD}(i)+\Gamma_D(i)$ does not equal unity since the resonance state i may also decay by autoionization into $H_2^+(\nu)$ without dissociation. This may cause vibrational cooling or heating of the molecular ions.

The ratio [Eq. (12)] is shown in the lower part of Fig. 5. It contains information about the autoionization probabilities, in particular below threshold for the direct vertical DE transitions since here, DE cannot proceed via direct excitation to the repulsive $(2p\sigma_u)\ ^2\Sigma_u^+$ dissociating curve. There are three structures in the ratio that peak at 6, 13, and at about 20 eV. The first is assigned to capture into the $(2p\sigma_u)nl\lambda$ manifold. The two other structures can be due to DE through direct transitions to the $(2p\sigma_u)\ ^2\Sigma_u^+$ and $(2p\pi_u)\ ^2\Pi_u$ states, respectively, as well as capture into autoionizing Rydberg states of the same core states [57]. It should be emphasized that systematic errors due to, for example, the ion-current measurement cancels when this ratio is considered. Thus, ratios obtained at different experiments can be compared, regardless of the normalization method applied, provided that an equal number of Rydberg states survive in the analyzing field (here $n_{max}=10$).

The DE cross section was recently calculated by Takagi [44,53] for energies below 10 eV using multichannel quantum-defect theory (MQDT). The first calculation [44] yielded a cross section that is about a factor of 2 smaller than our measurement. The new calculation [53] is in better agreement with the data as seen in Fig. 5, upper part. The ratio $\sigma_{DE}/(\sigma_{DE}+\sigma_{DR})$ as calculated by Takagi, is compared with the present data in the lower part of Fig. 5. Apparently, the first theoretical effort resulted in a peak position and width in relatively good agreement with the data, but the theoretical ratio is significantly lower than the experimental one mainly because of the small DE cross section in the calculation. In the latest MQDT calculation [53] the magnitude of the DE cross section is improved.

2. DR of HD^+

Absolute DR cross sections with vibrationally cold HD^+ have previously only been obtained by Strömholm *et al.* [26]. In their work as well as in other works [18,19,22] the cross section was found to exhibit narrow resonances at low energy ($E<1$ eV). This is attributed to interference between a direct DR process, involving a vertical transition from the initial ion state to a repulsive curve of the neutral molecule, and an indirect process, involving capture of the electron to a Rydberg state belonging to the initial ion potential curve, the energy gain being used to excite the vibrational motion of the nuclei. At higher energies, peaks were found at about 9 and 15 eV. They originate from excited Rydberg states of HD converging to the $2p\sigma_u$ and $2p\pi_u$ states (see Fig. 1). In the work by Stromholm *et al.* [26], the cross section at the peak at about 8–10 eV was compared with a MQDT calculation. Good agreement was obtained between theory and experiment when four symmetries [$^1\Sigma_g^+$ from $(2p\sigma_u)^2$ and $^1\Pi_g$, $^1\Sigma_u^+$, $^3\Pi_g$ from Rydberg states belonging to the $2p\sigma_u$ ion core] were included in the calculation. The complete dissociative Rydberg series for each molecular symmetry was included by introducing an effective state for the highest ($n>6$) Rydberg states. Thus, based on this work, it may seem that DR of the simplest molecular ion in this energy region is a solved problem.

At low energy (<0.1 eV) we obtain, as seen on Fig. 6, close agreement with the cross sections obtained at CRYRING [26]; despite the fact that calculations show that, due to different electron temperatures in the two experiments, the averaged cross section $\langle\sigma\rangle$ should differ by about 10–30% between 0.001 and 0.01 eV ($\langle\sigma\rangle$ obtained at CRYRING is expected to be largest due to a lower electron temperature). The difference is, however, within the uncertainty of the absolute calibration in the two experiments. Our DR cross sections in the high-energy region, where electron temperatures are indifferent to the magnitude of the cross section, are considerably larger than those obtained at CRYRING, as shown in Fig. 6. At the peak at about 9 eV, the ratio between the experimental data is 1.7.

Figure 7 shows the same experimental data as Fig. 6, except that the ASTRID data have been corrected for the contributions in the toroidal sections. Corrections for the TSR and CRYRING data are expected to be small owing to the higher ion energy applied in these measurements, and were not made. A significant discrepancy remains at the 9-eV peak and at higher energies. The MQDT calculations of Takagi [44,53] (theory I, II) are in close agreement with the present data at the cross-section peak, and the cross section below the peak is overestimated only in the first calculation. In the calculations by Takagi, five symmetries [$^1\Sigma_g^+$ from

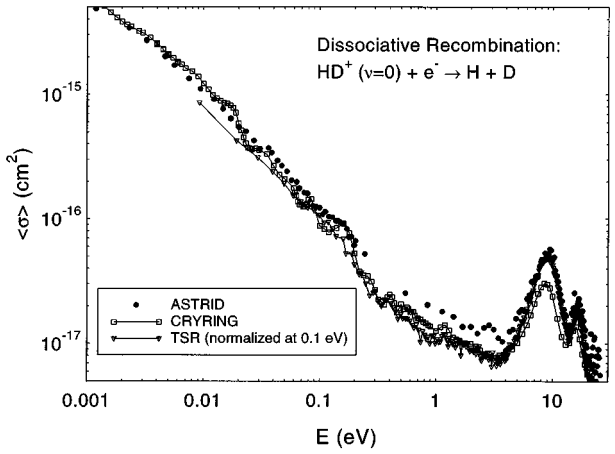

FIG. 6. Averaged DR cross sections $\langle\sigma\rangle=\langle v\sigma\rangle/v$ as a function of energy for HD^+. Shown are the absolute data of the present work together with the absolute data from CRYRING [26] and the relative data from TSR [20,57]. The TSR data were normalized to 0.8 times the present data at 0.1 eV to account for the different electron-beam temperatures. No correction for the contributions from the toroidal sections was made for the data on this figure. The difference at 1–5 eV, where the cross section is small, is caused by a large contribution from the toroide sections at the ASTRID experiment (see text and Fig. 7).

$(2p\sigma_u)^2$ and $^1\Sigma_g$, $^1\Pi_g$, $^1\Sigma_u$, $^3\Pi_g$, $^3\Pi_u$ from Rydberg states belonging to the $2p\sigma_u$ ion core] were included. They were all found to contribute significantly to the cross section. As seen in Fig. 7, the other MQDT calculation (theory III) [26] fits very well with the lower CRYRING data, but not with the present data.

In Figs. 6 and 7 we show for comparison the *relative* DR cross sections obtained at TSR [20]. The TSR data have been normalized to the ASTRID data at the energy of 0.1 eV. The TSR cross section at this energy is deliberately set to 80% of the cross section from the present work due to the different transverse electron temperatures in the two experiments (~0.1 eV at TSR and ~0.02 eV at ASTRID). The

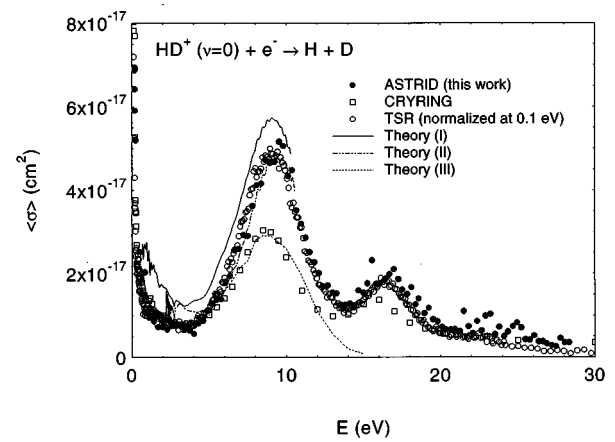

FIG. 7. Absolute DR cross section of HD^+. Data from the present work are compared with data from CRYRING [26]. Also shown are results of MQDT calculations of Ref. [44] (theory I), Ref. [53] (theory II), and Ref. [26] (theory III). Only the ASTRID data have been corrected for contributions from the toroidal regions.

normalized DR data from TSR are consistent with the ASTRID data over the entire energy range.

A possible source for some of the discrepancy between the ASTRID and CRYRING data may be a different amount of stripping of Rydberg states in the bending magnets. In the present experiment $n_{max}=10$, but n_{max} equaled only 7 in the experiment of Strömholm *et al.* [26], which resulted in a smaller cross section since high Rydberg states $n>4$ are involved in the DR process at high energy [23]. The issue of stripping of Rydberg states was not considered in the paper by Stromholm *et al.* [26]. Rotational differences in the two ion beams are not expected to be significant. The two MQDT calculations [26,44] yield cross sections that differ by about a factor of 2 at the peak at ~9 eV. The difference may be due to inclusion of different molecular states in the calculations, the treatment of the off-the-energy shell effects, the applied autoionization probabilities and the treatment of Rydberg states.

B. Imaging of H_2^+

It is difficult to compare DR data of H_2^+ from different experiments since the vibrational and rotational distributions may vary greatly between the experiments and, moreover, it has been difficult to obtain information about these distributions. Once the molecular ions are created in vibrationally and rotationally excited levels in the ion source, they do not easily cool down. In storage rings, where ions are stored for many seconds, some relaxation may occur due to collisions with the background gas. Some of the very highly vibrationally excited ions, which are probably not produced in any great amount in the ion source, may stabilize due to dipole transitions induced by strong external fields that may polarize the molecule, or field dissociation may destroy ions in these levels. By comparing DR spectra recorded at different times after production and injection into the storage ring, we see very little relaxation of the H_2^+ ions, which means that such passive cooling schemes are rather ineffective for the conditions at ASTRID. It is interesting to note that the H_2^+ beam obtained at CRYRING [25] seems to be much colder than the one obtained at ASTRID. This may be due to the fact that the ions in CRYRING were merged with electrons at $E=0$ (cooling) for about 20 s before the measurement took place. During the cooling period, an ion may capture an electron, but rather than dissociate, it may autoionize not only to the same initial vibrational level but also to lower vibrational levels and hence cause vibrational cooling. In ASTRID the cooling period was at most a few seconds; hence, this possible cooling effect would be much smaller here. Different ion-source conditions may also explain the difference.

We used photodissociation [Eq. (3)] to actively manipulate the vibrational distribution of the stored ions and the imaging technique to measure the change of the vibrational distribution. The imaging technique also provided information about the final electronic states of the hydrogen atoms, an issue that has been addressed before [15,58,59]. As seen in Fig. 8, there is a significant difference between the data recorded when the laser is off and that recorded with the laser on (from the time of injection to the end of the measurement 30 s later). The imaging data, yield *versus* pro-

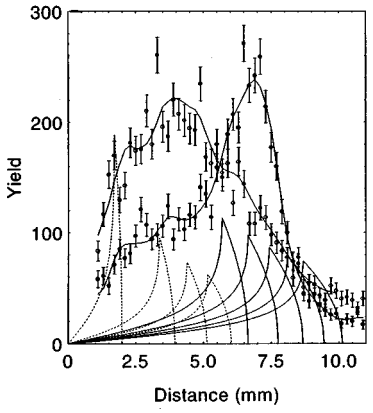

FIG. 8. Yield of pairs of H atoms following DR with H_2^+ as a function of the projected distance on the detector, recorded at $E=0$. Data recorded with the laser on (solid circles) is compared with data recorded with the laser being off (open circles). Dashed lines are calculated contributions (arbitrary scale) of the $H(n=1)+H(n=3)$ channel from different vibrational levels ($\nu=5$–8) without inclusion of rotations. Solid lines are calculations of the $H(n=1)+H(n=2)$ channels ($\nu=0$–4, $J=0$). No sign of the $H(n=1)+H(n=1)$ channel was seen. Solid lines through the data are fits including rotational excitation.

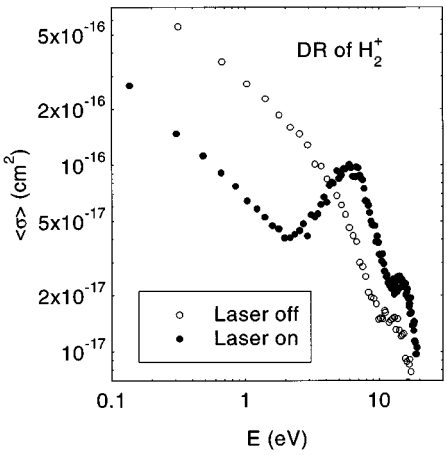

FIG. 9. Dissociative-recombination cross sections for H_2^+ as a function of energy for hot and cold H_2^+. The cross sections are corrected for the toroid contribution.

jected distance between H atoms, display two main structures that may be related to the population of hydrogen atoms in two different electronic configurations (channels). The peak below 6 mm is primarily due to the $H(n=1)+H(n=3)$ channel, which is energetically allowed for $\nu\geqslant 5$ ($J=0$). This peak is significantly reduced when the laser is turned on. The second peak structure between 5 and 9 mm is due to the $H(n=1)+H(n=2)$ channel, which is open for all vibrational levels. When the laser is on this peak has contributions only from the lowest vibrational levels of H_2^+. The $H(n=1)+H(n=1)$ channel has an expected peak position at about 20 mm. However, we see no evidence of this channel in the data.

In the case of HD^+, the imaging spectrum (Fig. 4) exhibited a single sharp peak that was attributed to one vibrational level ($\nu=0$) without invoking rotations; i.e., the beam was rotationally cold. It is evident that the imaging spectra of Fig. 8 do not exhibit sharp peaks due to individual vibrational levels. Rotational excitation causes a ''smearing'' of the data. We have seen the same effect in imaging data of $^{15}N^{14}N^+$ [4] where, due to only a small dipole moment, the nitrogen molecular ions were rotationally hot. The solid curves through the data in Fig. 8 represent fits to the data with the function $D(R)$ given in Eq. (10), which includes rotations. The fits yield a rotational temperature that is around 0.1–0.2 eV. When the laser is off, $P(\nu,f)$ is significant for all vibrational levels up to $\nu=7$. With the laser on, $P(\nu,f)$ has contributions primarily from $\nu=0$ and 1 for the $H(n=1)+H(n=2)$ channel, in good agreement with the estimates based on the applied laser power and known dissociation cross sections (see Fig. 3). We find that for the sum of $P(\nu,f)$ for $\nu=2$–5 of the $H(n=1)+H(n=2)$ channel is reduced by a factor of 4 when the laser is turned on and the sum of $P(\nu,f)$ for $\nu=5$–8 of the $H(n=1)+H(n=3)$ channel is reduced by more than a factor of 10. We find that even with the laser on $P(5,f)$ and $P(6,f)$ are non-negligible for the $H(n=1)+H(n=3)$ channel, indicating that the DR cross section for this channel is much larger than that of the $H(n=1)+H(n=2)$ channel when energetically allowed. The $\nu=5$ and 6 contributions to the imaging spectrum taken with the laser on are noticed as small humps on the data at projected distances below 5 mm; see Fig. 8. The rotational energy $kT\sim 0.1$–0.2 eV is of the same magnitude as that obtained with $^{15}N^{14}N^+$ [4] and seems reasonable for the type of ion source used.

Since $P(\nu,f)$ is the product of the vibrational population and the cross section, we cannot at the same time obtain information about the vibrational dependence of the DR cross section and the vibrational population of the beam. One might assume an initial Frank-Condon type of vibrational distribution. However, the statistical uncertainty of the fitting parameters from the present data does not allow a prediction of the vibrational dependence of the cross section based on such assumptions.

1. DR of H_2^+

The dissociative-recombination cross sections for hot and cold H_2^+ are shown in Fig. 9. Note that these data were recorded under exactly equal conditions, except for the presence of the laser light. The cross section obtained with the hot beam has hardly any structure. The many vibrational levels simply smear out the resonant character of the DR reaction [9]. When vibrational cooling is applied, the cross section is reduced at low energy, and at high energy structures are obtained similar to those obtained for HD^+. This by itself shows that cooling has taken place [9,11]. The DR cross section of $H_2^+(\nu=0,1)$ is larger than that of $HD^+(\nu=0)$ by a factor of 2–5, which indicates that the $\nu=1$ cross section is significantly larger than that of $\nu=0$. It is also seen that the peak at 5–9 eV is more extended towards low energy for $H_2^+(\nu=0,1)$ than for $HD^+(\nu=0)$, in accordance with expectations since $\nu=1$ contributes at a lower energy than $\nu=0$ does. In fact the experimental DR cross section for HD^+ peaks at $\sim$9 eV, which is the position of the $2p\sigma_u\,(^2\Sigma_u^+)nl\lambda$ Rydberg resonances for $\nu=0$ predicted by a simple Franck-Condon factor based calculation [9]. The

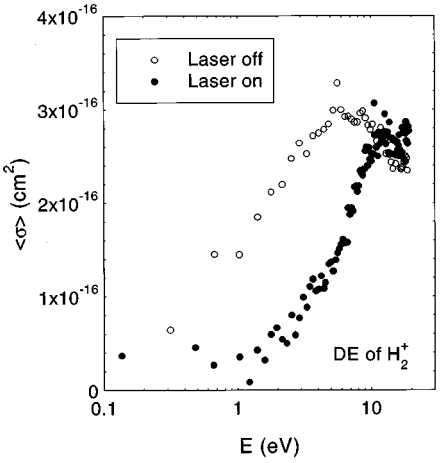

FIG. 10. Dissociative-excitation cross sections for H_2^+ as a function of energy for hot and cold H_2^+. The cross sections are corrected for the toroid contribution.

laser-cooled H_2^+ spectrum peaks at ~6 eV, where the same calculation predicts the $\nu=1$ peak to have its maximum. The present cross sections obtained with uncooled ions are somewhat lower (by about a factor of 2–3) than those obtained in earlier works (see Refs. [60,61]); presumably due to a different vibrational distribution. The cross sections obtained with cold H_2^+ are in reasonable agreement with early low-energy, low-statistics data of Hus *et al.* [18].

2. DE of H_2^+

The DE cross section as a function of energy for H_2^+ is shown in Fig. 10. It is first noted that the DE cross section is significant below the energy of the vertical $(1s\sigma_g)\ ^2\Sigma_g^+$-$(2p\sigma_u)\ ^2\Sigma_g^+$ transition indicating that, as for HD^+, the process may proceed via electron capture to doubly excited states of the neutral molecule, followed by autoionization and dissociation. The cross section vanishes at low energy for both the cold and the hot molecular ions. We know that vibrational levels up to $\nu=7$ are present in our hot H_2^+ beam from the imaging data, and the low-energy cutoff in the DE data at about 0.1–0.2 eV indicates that only $\nu<13$ is present in any significant amount.

Yousif and Mitchell [42] found that the DE cross section below 0.1 eV was as large as 10^{-15}–10^{-14} cm^2 with an assumed vibrational distribution similar to a Franck-Condon distribution. We have no reason to believe that our vibrational distribution for the uncooled beam is very different from a Franck-Condon distribution. The difference between the present data and previous data [42,47] is not immediately understood. The size of the cross section at our maximum agrees within a factor of 2–3 with that obtained by other groups with hot ions (see, for example, the data collected in Ref. [42]).

When the laser is on, the threshold is significantly shifted toward higher energy, as expected. The energy required to dissociate the $H_2^+(J=0)$ molecular ion is 2.65 eV from $\nu=0$, 2.38 eV from $\nu=1$, and 2.12 eV from $\nu=2$. The energy thresholds are lower by about 0.2 eV when the rotational excitation is taken into account. Indeed, the cross section starts to increase at about the expected 2 eV, corresponding to a beam with mainly $\nu=0$ and 1 populated. The cross section obtained with the cold beam has a maximum value of about the same magnitude as that obtained with the hot beam. This shows that beams with significantly different vibrational distributions may result in DE cross sections that are comparable in magnitude in the high-energy region (>10 eV).

The DE cross section of H_2^+ in the $\nu=0$ and $\nu=1$ states can be estimated in the following way. We assume that the cross sections for H_2^+ and HD^+ for $\nu=0$ are identical and the presence of small amounts of ions in other vibrational levels ($\nu>1$) in the cooled H_2^+ beam can be ignored. If the relative $\nu=0$ to $\nu=1$ population in the beam is 1:1 the cross-section ratio $\sigma(\nu=0)/\sigma(\nu=1)$ is from the data found to be 1/3 at around 10–20 eV. If the population ratio is closer to that of a Franck-Condon distribution, for example, 3:7, the same cross-section ratio is about 2/5. Thus, the data may indicate that the DE cross section at 10–20 eV involving ions in the first vibrationally excited state is larger than that involving ions in the vibrational ground state.

IV. CONCLUSION

In the present work, we studied DE and DR for the HD^+ and H_2^+ molecular hydrogen ions. By the use of a laser and long storage times we were able to manipulate the vibrational distribution of the H_2^+ ions and obtain a beam with mainly $\nu=0$ and $\nu=1$ populated. Without the application of the laser many vibrational states of the H_2^+ ions were populated. It was found that rotational excitation must be considered for H_2^+. The HD^+ beam was found to be vibrationally and rotationally cold.

With these molecular ions absolute DE and DR cross sections as a function of energy from 0 to ~30 eV was measured. An imaging technique was used to probe the initial and final states of the particles involved. With $HD^+(\nu=0)$ and electrons at zero kinetic energy, only the $H(n=1)+D(n=2)$ $[H(n=2)+D(n=1)]$ channel contributes to the DR reaction. For H_2^+ and electrons at zero kinetic energy, both the $H(n=1)+H(n=2)$ channel and the $H(n=1)+H(n=3)$ channel contribute to the DR reaction, though the latter does so only from vibrationally excited levels ($\nu\geqslant 5$). The absolute DR cross sections of HD^+ were compared with experimental data from other storage rings and a discrepancy was found at high energy, where also MQDT calculations yield different results. This shows that the DR of HD^+, which based on a recent paper [26] might appear as an essentially solved problem, is not completely understood and further investigations are needed.

The DE cross sections exhibited a threshold at an energy smaller than the energy difference between the initial ion curve and the first repulsive ion curve. The description of DE should therefore include electron capture with subsequent autoionization and dissociation. The DE and DR cross sections of H_2^+ were sensitive to the initial vibrational distribution and the data indicated that the cross sections for vibrationally excited ions ($\nu=1$) are larger than those for ions in the vibrational ground state.

ACKNOWLEDGMENTS

This work has been supported by the Danish National Research Foundation through the Aarhus Center for Advanced Physics (ACAP). We thank Poul Kristensen for help-with the laser used in this experiment and the ASTRID staff for providing the high-energy ion beam needed. The TSR and CRYRING groups are acknowledged for providing us with their experimental data and Hidekazu Takagi for files containing the MQDT calculations. One of us (L.H.A) thanks JILA, University of Colorado for hospitality.

[1] S. L. Guberman and A. Giusti-Suzor, J. Chem. Phys. **95**, 2602 (1991).
[2] Cross sections and branching ratios have been obtained at ASTRID, D. Kella, L. Vejby-Christensen, P. J. Johnson, H. B. Pedersen, and L. H. Andersen (unpublished).
[3] J. L. Fox, J. Geophys. Res. **98**, 3297 (1993).
[4] D. Kella, P. J. Johnson, H. B. Pedersen, L. Vejby-Christensen, and L. H. Andersen, Phys. Rev. Lett. **77**, 2432 (1996).
[5] S. Datz *et al.*, Phys. Rev. Lett. **74**, 896 (1995).
[6] L. H. Andersen *et al.*, Phys. Rev. Lett. **77**, 4891 (1996).
[7] M. Larsson, Rep. Prog. Phys. **58**, 1267 (1995).
[8] H. Danared *et al.*, Phys. Rev. Lett. **72**, 3775 (1994).
[9] H. T. Schmidt, L. Vejby-Christensen, H. B. Pedersen, D. Kella, N. Bjerre, and L. H. Andersen, J. Phys. B **29**, 2485 (1996).
[10] C. H. Greene and B. Yoo, J. Phys. Chem. **99**, 1711 (1995); S. Guberman, J. Chem. Phys. **78**, 1404 (1983); T. E. Sharp, At. Data **2**, 124 (1970).
[11] M. Larsson *et al.*, J. Phys. B **27**, 1397 (1994).
[12] F. Von Busch and G. H. Dunn, Phys. Rev. A **5**, 1726 (1972).
[13] B. Peart and K. T. Dolder, J. Phys. B **6**, L359 (1973).
[14] B. Peart and K. T. Dolder, J. Phys. B **7**, 236 (1974).
[15] R. A. Phaneuf, D. H. Crandall, and G. H. Dunn, Phys. Rev. A **11**, 528 (1975).
[16] D. Auerbach *et al.*, L. Phys. B **10**, 3797 (1977).
[17] D. Mathur, S. U. Khan, and J. B. Hasted, J. Phys. B **11**, 3615 (1978).
[18] H. Hus, F. Yousif, C. Noren, A. Sen, and J. B. A. Mitchell, Phys. Rev. Lett. **11**, 1006 (1988).
[19] P. Van der Donk, F. B. Yousif, J. B. A. Mitchell, and A. P. Hickman, Phys. Rev. Lett. **67**, 42 (1991).
[20] P. Forck *et al.*, Phys. Rev. Lett. **70**, 426 (1993).
[21] P. Forck *et al.*, Nucl. Instrum. Methods B **79**, 273 (1993).
[22] T. Tanabe *et al.*, Phys. Rev. Lett. **74**, 1066 (1995).
[23] D. Zajfman *et al.*, Phys. Rev. Lett. **75**, 814 (1995).
[24] D. Zajfman *et al.*, *XVIII International Conference on the Physics of Electronic and Atomic Collisions, Abstracts of Contributed Papers*, edited by T. Andersen, B. Fastrap, F. Folkmann, and H. Knudsen (IFA, Aarhus University, Aarhus, 1993), Vol. 1, p. 383.
[25] M. Larsson *et al.*, Phys. Scr. **51**, 354 (1995).
[26] C. Strömholm *et al.*, Phys. Rev. A **52**, R4320 (1995).
[27] V. P. Zhdanov and M. I. Chibisov, Zh. Eksp. Teor Fiz. **74**, 75 (1978) [Sov. Phys. JETP **47**, 38 (1978)].
[28] C. Derkits, J. N. Bardsley, and J. M. Wadehra, J. Phys. B **12**, L529 (1979).
[29] V. P. Zhdanov, J. Phys. B **13**, L311 (1980).
[30] A. Giusti-Suzor, J. N. Bardsley, and C. Derkits, Phys. Rev. A **28**, 682 (1983).
[31] K. Nakashima, H. Takagi, and H. Nakamura, J. Chem. Phys. **86**, 726 (1987).
[32] A. P. Hickman, J. Phys. B **20**, 2091 (1987).
[33] I. F. Schneider, O. Dulieu, and A. Giusti-Suzor, J. Phys. B **24**, L289 (1991).
[34] H. Takagi, J. Phys. B **26**, 4815 (1993).
[35] I. F. Schneider, O. Dulieu, and A. Giusti-Suzor, Phys. Rev. Lett. **68**, 2251 (1992).
[36] A. P. Hickman, in *Dissociative Recombination: Theory, Experiment and Applications*, edited by J. B. A. Mitchell and S. Guberman (World Scientific, Singapore, 1989), p. 73.
[37] G. H. Dunn, B. Van Zyl, and R. N. Zare, Phys. Rev. Lett. **15**, 610 (1965).
[38] D. F. Dance *et al.*, Proc. Phys. Soc. **92**, 577 (1967).
[39] G. H. Dunn and B. van Zyl, Phys. Rev. **154**, 40 (1967).
[40] B. Peart and K. T. Dolder, J. Phys. B **5**, 860 (1972).
[41] B. Peart and K. T. Dolder, J. Phys. B **5**, 1554 (1972).
[42] F. B. Yousif and J. B. A. Mitchell, Z. Phys. D **34**, 195 (1995).
[43] D. Mathur, J. B. Hasted, and S. U. Khan, J. Phys. B **12**, 2043 (1979).
[44] H. Takagi, in *Proceedings of the 1995 Workshop on Dissociative Recombination: Theory, Experiment and Application III*, edited by D. Zajfman *et al.* (World Scientific, Singapore, 1996), p. 174.
[45] J. M. Peek, Phys. Rev. **154**, 52 (1967).
[46] S. P. Møller, in *Conference Record of the 1991 IEEE Particle Accelerator Conference, San Francisco*, edited by K. Berkner (IEEE, New York, 1991), p. 2811.
[47] K. O. Nielsen, Nucl. Instrum. Methods **1**, 289 (1957).
[48] L. H. Andersen, J. Bolko, and P. Kvistgaard, Phys. Rev. A **41**, 1293 (1990).
[49] L. Vejby-Christensen, L. H. Andersen, D. Kella, D. Mathur, H. B. Pedersen, and H. T. Schmidt, Phys. Rev. A **53**, 2811 (1996).
[50] G. H. Dunn, Phys. Rev. **172**, 1 (1968); G. H. Dunn, JILA Report No. 92, 1968 (unpublished)
[51] F. Von Busch and G. H. Dunn, Phys. Rev. A **5**, 1726 (1972).
[52] L. Landau and E. Lifshitz, *The Classical Theory of Fields* (Addison-Wesley, New York, 1951).
[53] A new MQDT calculation was communicated to us by H. Takagi.
[54] G. Hunter, A. W. Yau, and H. O. Pritchard, At. Data Nucl. Data Tables **14**, 11 (1974).
[55] L. J. Kieffer and G. H. Dunn, Phys. Rev. **158**, 61 (1967).
[56] A. U. Hazi, Chem. Phys. Lett. **25**, 259 (1974).
[57] D. Zajfman *et al.*, in *Proceedings of the 1995 Workshop on Dissociative Recombination: Theory, Experiment and Application III*, edited by D. Zajfman *et al.* (World Scientific, Singapore, 1996), p. 114.
[58] C. Strömholm (private communication).
[59] M. Vogel and G. H. Dunn, Phys. Rev. A **11**, 1983 (1975).
[60] J. B. A. Mitchell *et al.* (unpublished).
[61] J. B. A. Mitchell, in *Proceedings of the 1995 Workshop on Dissociative Recombination: Theory, Experiment and Application III* (Ref. [44]), p. 21.